second zinc-binding sites within the RING domain of AGM TRIM5α were replaced with alanine residues, respectively. All mutant TRIM5α constructs contained the HA-tag at their C-terminus (Fig. 1C).

To determine the effects of TRIM5α RING mutations on its ubiquitin ligase activity, 293 T cells were transfected with plasmids encoding HA-tagged TRIM5αs together with plasmid expressing myc tagged ubiquitin. Forty-eight hours later, the cells were lysed and TRIM5α proteins were precipitated with the anti-HA antibody followed by Western blot analysis using anti-HA and anti-myc antibodies. Poly-ubiquitinated forms of the wild type AGM TRIM5α were observed (Fig. 1D). AGM TRIM5α with C15AC18A or C30AH32A was less poly-ubiquitinated than the wild type AGM TRIM5α, and AGM TRIM5α with C15AC18AC30AH32A was the least poly-ubiquitinated among the mutant constructs tested. These results confirmed the previously published report (Diaz-Griffero et al., 2006) that the TRIM5α RING zinc-binding site mutations impaired auto poly-ubiquitination of TRIM5α.

Contribution of RING domain to retrovirus restriction by AGM TRIM5α

We next examined anti-viral activities of zinc-binding site mutants of TRIM5α. The HA-tagged wild type and mutant AGM TRIM5α proteins were expressed by SeVs in MT4 cells (Fig. 2A). CV1 cells were then used for a confocal microscopic examination of cytoplasmic bodies, since the cytoplasm of MT4 cells is not large enough for observation of cytoplasmic bodies. Each of the TRIM5αs with RING mutations formed uniformly larger cytoplasmic bodies than did the wild type (Fig. 2B), although the size of cytoplasmic bodies slightly

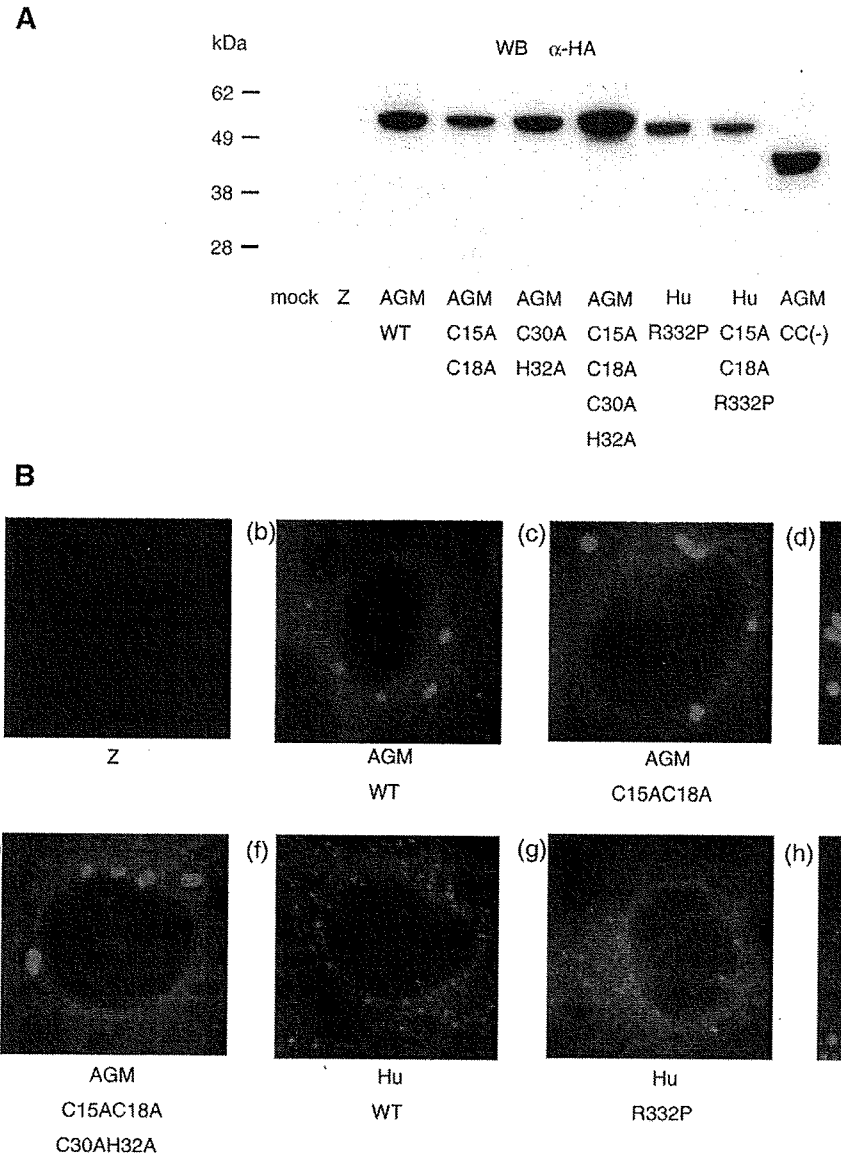

Fig. 2. Expression of RING mutant TRIM5α proteins. (A) Expression of various TRIM5αs. TRIM5α proteins in MT4 cells mock infected (mock) or infected with parental Z strain of SeV (Z), SeVs expressing AGM TRIM5α (AGM WT), AGM TRIM5α C15AC18A (AGM C15AC18A), AGM TRIM5α C30AH32A (AGM C30AH32A), AGM TRIM5α C15AC18AC30AH32A (AGM C15AC18AC30AH32A), human TRIM5α R332P (Hu R332P), human TRIM5α C15AC18AR332P (Hu C15AC18AR332P), or AGM-TRIM5α-Coiled-coil(—) (AGM CC(—)), were visualized by Western blotting with antibody to HA. (B) Subcellular localization of TRIM5αs. CV1 cells infected with SeV expressing HA-tagged TRIM5 proteins were analyzed as described in "Materials and methods". Representative confocal microscopic images are shown of parental Z strain of SeV (a), or with SeV expressing AGM WT (b), AGM C15AC18A (c), AGM C30AH32A (d), AGM C15AC18AC30AH32A (e), Hu WT (f), Hu R332P (g), or Hu C15AC18AR332P (h).

Please cite this article as: Maegawa, H., et al., Contribution of RING domain to retrovirus restriction by TRIM5α depends on combination of host and virus, Virology (2010), doi:10.1016/j.virol.2010.01.003

varied among different RING mutants of TRIM5α. These results confirmed the previous observations on Rh TRIM5α (Javanbakht et al., 2005). Specifically, AGM TRIM5α with C30AH32A showed the highest numbers of cytoplasmic bodies and the least levels of diffuse staining of cytoplasm among the three RING mutants (Fig. 2B).

For the viral replication assay, MT4 cells infected with SeVs expressing the wild type and mutant TRIM5αs were also superinfected with the NL43 strain of HIV-1, GH123 strain of HIV-2 or SIVmac239. Three days after infection, culture supernatants were collected and assayed for their levels of p24, p25 or p27 viral CA protein, respectively. AGM-TRIM5α-CC(−) was used as a negative control. AGM TRIM5α with C15AC18A, C30AH32A, or C15AC18A-C30AH32A moderately inhibited HIV-1 growth, while these variants completely lost their inhibitory effect on SIVmac growth (Fig. 3A). These results indicated that effects of cysteine substitutions in RING domain on anti-HIV-1 activity of AGM TRIM5α differ from those on anti-SIVmac activity, suggesting that SIVmac restriction by AGM TRIM5α was totally dependent on the intact RING domain of TRIM5α, while HIV-1 restriction was at least in part independent from this domain as reported previously (Javanbakht et al., 2005; Perez-Caballero et al., 2005b; Stremlau et al., 2004). It has been proposed that both proteasome-dependent and -independent pathways are involved in HIV-1 restriction by Rh TRIM5α, since disrupting the proteasome function by adding a proteasome inhibitor enabled the generation of normal levels of HIV-1 late reverse transcribed products, although HIV-1 infection and the generation of nuclear imports of 1-LTR and 2-LTR viral cDNA forms remained impaired by Rh TRIM5α (Anderson et al., 2006; Wu et al., 2006). We therefore concluded that AGM TRIM5α restricts SIVmac mainly via the RING-proteasome-dependent pathway.

We then tested the third virus, human immunodeficiency virus type 2 (HIV-2), which is more closely related to SIVmac than to HIV-1 (Gao et al., 1999). AGM TRIM5α clearly inhibited HIV-2 GH123 replication and all the RING domain mutants showed reduced anti-HIV-2 activity. AGM TRIM5α with C30AH32A completely lost its anti-HIV-2 activity (Fig. 3A). Unlike SIVmac, however, AGM TRIM5α with C15AC18A or C15AC18AC30AH32A still moderately inhibited HIV-2 GH123 growth (Fig. 3A). These results indicate that the RING domain contribution to HIV-2 restriction by TRIM5α was also distinct from its contributions to HIV-1 and SIVmac restrictions.

In a single round infection assay, MT4 cells infected with SeVs expressing the wild type or mutant TRIM5αs variants were superinfected with HIV-1-GFP or SIVmac-GFP. The wild type AGM TRIM5α potently restricted both HIV-1-GFP and SIVmac-GFP infection (Fig. 3B) as reported previously (Nakayama et al., 2005). On the other hand, AGM TRIM5α with C15AC18A, C30AH32A, or C15AC18A-C30AH32A only moderately inhibited HIV-1-GFP infection, while these variants completely lost their inhibitory effect on SIVmac-GFP infection (Fig. 3B). AGM C30AH32A exhibited the weakest anti-HIV-1 activity among the generated mutant constructs, probably due to its limited localization within the cytoplasm. However, the number of HIV-1-infected cells was still lower in AGM C30AH32A expressing cells than in those expressing negative control AGM-TRIM5α-CC(-) or cells infected with the parental SeV Z strain (Fig. 3B). The same results as above were obtained when we use canine Cf2Th cell line lacking endogenous TRIM5α expression (Sawyer et al., 2007) (Fig. 3C). These results confirmed our results in viral replication assay described in Fig. 3A.

Contribution of RING domain to retrovirus restriction by human TRIM5α with arginine-to-proline substitution at the 332nd position

An arginine-to-proline substitution at the 332nd position (R332P) in the SPRY domain reportedly conferred strong anti-HIV-1 and anti-SIVmac activities to human TRIM5α (Stremlau et al., 2005; Yap et al., 2005). To determine whether cystein residue substitutions in the RING domain of human TRIM5α with R332P (Hu-R332P) have similar effects on its anti-HIV-1 and anti-SIVmac activities to those of AGM TRIM5α described above, C15AC18A substitutions were introduced in Hu-R332P. The protein expression levels of Hu-R332P with C15AC18A were comparable to those of Hu-R332P without C15AC18A (Fig. 2B). In addition, Hu-R332P inhibited both HIV-1 and SIVmac infection (Fig. 3A, B and C), which confirmed previous findings (Stremlau et al., 2005; Yap et al., 2005). As expected, Hu-R332P with C15AC18A completely lost its auto poly-ubiquitination (Fig. 1D) and anti-SIVmac activity (Fig. 3A, B and C) indicating that SIVmac restriction by Hu-R332P also strongly depends on the intact RING domain of TRIM5α. In contrast to AGM TRIM5α, however, Hu-R332P with C15AC18A completely lost its anti-HIV-1 activity (Fig. 3A, B and C). These findings suggest that, unlike AGM TRIM5α, Hu-R332P TRIM5α restricted both HIV-1 and SIVmac mainly via a RING-proteasome-dependent pathway. Hu-R332P TRIM5α with C15AC18A also failed to restrict HIV-2 GH123 (Fig. 3A). Taken together with results on AGM TRIM5α described above, our results indicated that the extent of RING domain contribution to retrovirus restriction by TRIM5α could be determined by a combination of virus and host species. We speculate that the intact RING domain is required for the proteasome-dependent but not for the proteasome-independent pathway of TRIM5α restriction of retroviruses.

Effect of proteasome inhibition on antiviral activity of TRIM5α

For a direct investigation of whether AGM TRIM5α restricts SIVmac and Hu-R332P TRIM5α restricts both HIV-1 and SIVmac mainly via proteasome-dependent pathway, we used a proteasome inhibitor MG132. MT4 cells infected with SeVs expressing various TRIM5α were superinfected with HIV-1-GFP or SIVmac-GFP in the presence or absence of MG132. After infection, the cells were thoroughly washed and incubated in MG132-free medium. As shown in Fig. 4, MG132 had no effect at all on the anti-HIV-1 activity of AGM, Rh or cynomolgus monkey and of human/AGM chimeric TRIM5α carrying the SPRY domain of AGM TRIM5α and the RING, B-box 2, and coiled-coil domains of human TRIM5α. In contrast, and as expected, MG132 at least partially disrupted the anti-HIV-1 activity of Hu-R332P TRIM5α. Rh and cynomolgus monkey TRIM5α could not restrict SIVmac infection and that addition of MG132 did not affect the numbers of GFP-positive cells, indicating that the condition for MG132 treatment used in our study did not affect cell viability (Fig. 4). AGM, Hu-R332P and human/AGM chimeric TRIM5α restricted SIVmac infection while MG132 partially disrupted the anti-SIVmac activity of those TRIM5α. When we used Cf2Th cells, MG132 also disrupted the anti-HIV-1 activity of Hu-R332P TRIM5α at least

Fig. 3. Contribution by RING domain to retrovirus restriction by TRIM5α depends on combination of host and viral species. (A) MT4 cells were infected with SeV expressing AGM CC (−), AGM WT, AGM C15AC18A, AGM C30AH32A, AGM C15AC18AC30AH32A, Hu R332P, or Hu C15AC18AR332P. The cells were then superinfected with HIV-1 NL43, HIV-2 GH123 or SIVmac239. The culture supernatants were collected three days after infection for measurement of the p24, p25 or p27 levels. The representative results of two independent experiments with similar results are shown. Error bars denote actual fluctuations of duplicate samples. (B) MT4 cells were infected with parental Z strain of SeV (crosses), or with SeVs expressing AGM WT (black squares), AGM CC(−) (white squares), AGM C15AC18A (black triangles), AGM C30AH32A (white triangles), AGM C15AC18AC30AH32A (white diamonds), Hu R332P (black circles), or Hu C15AC18AR332P (white circles). The cells were then superinfected with serially diluted HIV-1-GFP or SIVmac-GFP. The representative results of two independent experiments with similar results are shown. (C) Canine Cf2Th cells were infected with SeVs expressing indicated TRIM5α protein. The cells were then superinfected with HIV-1-GFP or SIVmac-GFP. The representative results of four independent experiments with similar results are shown. Error bars denote standard deviation in triplicate samples.

Please cite this article as: Maegawa, H., et al., Contribution of RING domain to retrovirus restriction by TRIM5α depends on combination of host and virus, Virology (2010), doi:10.1016/j.virol.2010.01.003

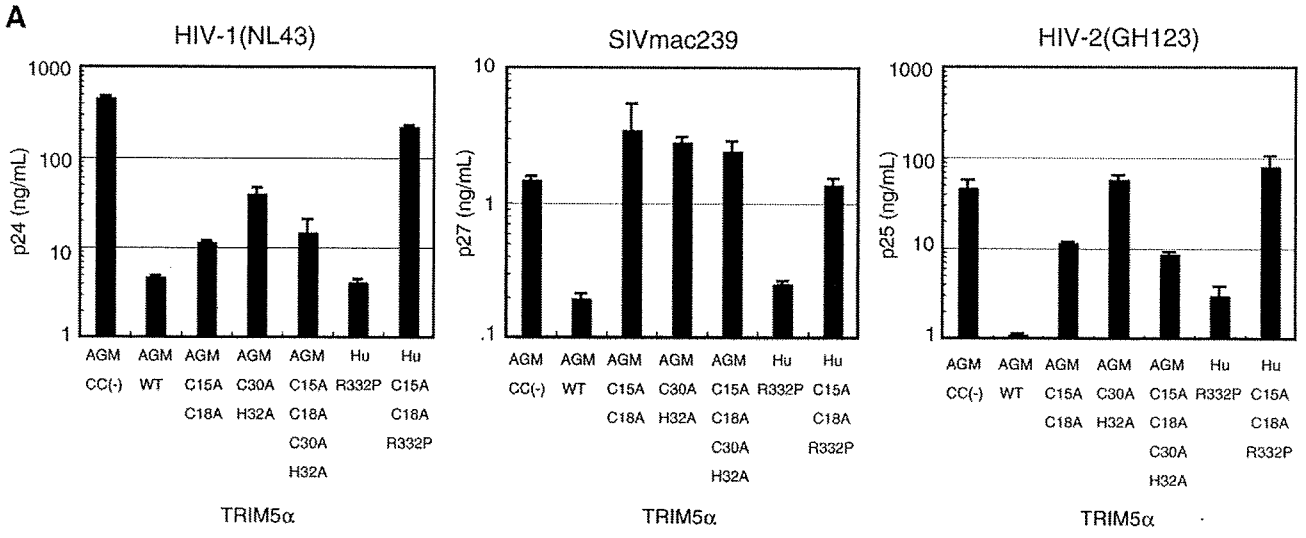

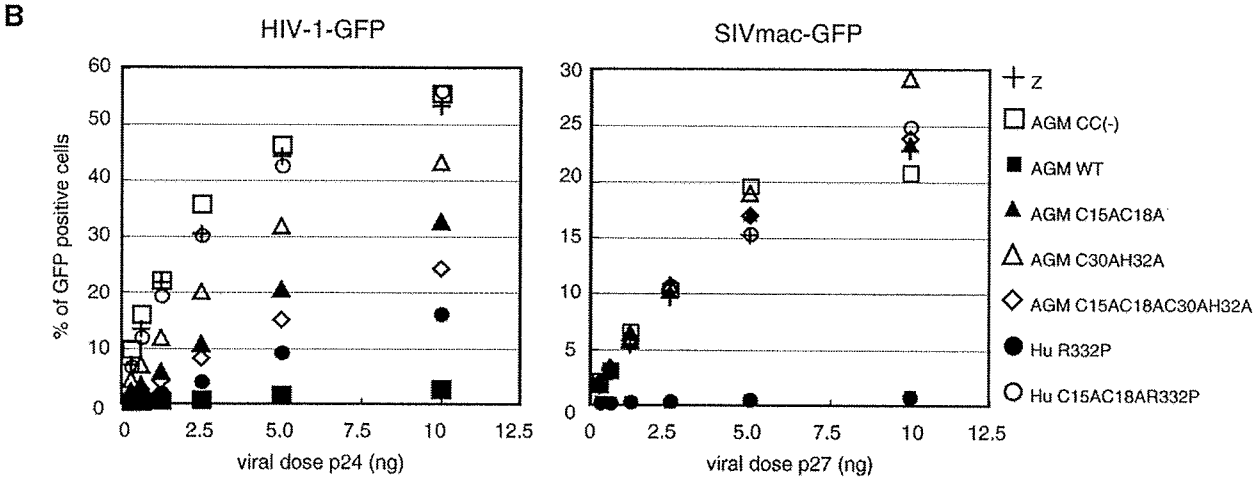

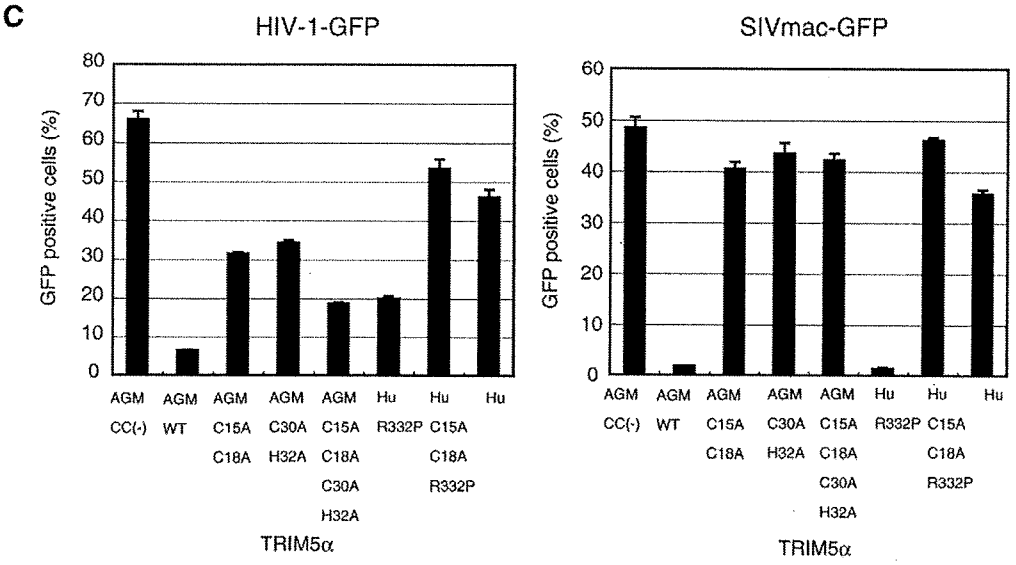

Please cite this article as: Maegawa, H., et al., Contribution of RING domain to retrovirus restriction by TRIM5α depends on combination of host and virus, Virology (2010), doi:10.1016/j.virol.2010.01.003

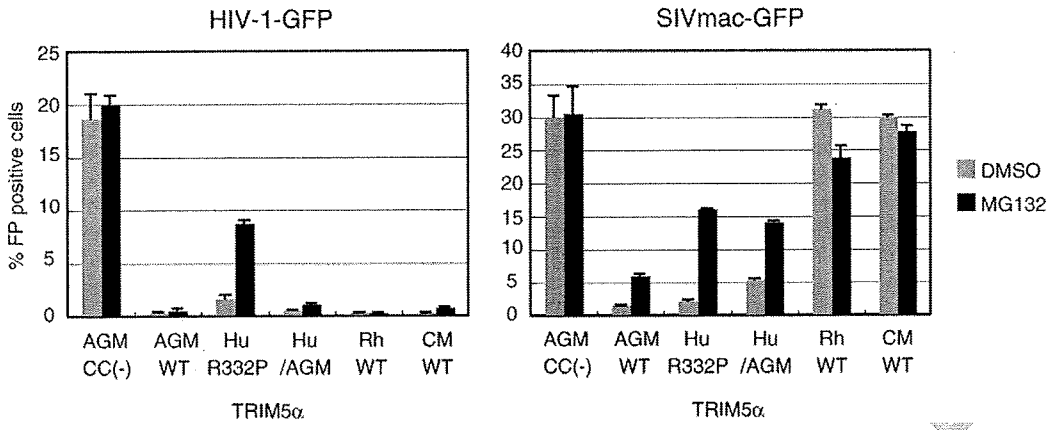

Fig. 4. The effect of proteasome inhibition on antiviral activity of TRIM5α depends on combinations of TRIM5α and viruses. MT4 cells were infected with SeVs expressing AGM CC (−), AGM WT, Hu R332P, Hu/AGM, Rh WT or CM WT. Cells were then superinfected with HIV-1-GFP or SIVmac-GFP in the presence of 10 μM MG132 in 0.1% DMSO (black bar) or 0.1% DMSO (gray bar). The representative results of three independent experiments with similar results are shown. Error bars denote actual fluctuations of duplicate samples.

partially (data not shown). These results support our conclusions that AGM TRIM5α restricted SIVmac mainly via the proteasome-dependent pathway, and that Hu-R332P TRIM5α restricted both HIV-1 and SIVmac mainly via the proteasome-dependent pathway (see Table 1 for summary of these results).

As described above, the previous studies have shown that disrupting the proteasome function by adding a proteasome inhibitor enabled the generation of HIV-1 late reverse transcribed products, even though HIV-1 infection and the generation of nuclear imports of 1-LTR and 2-LTR viral cDNA forms remained impaired by Rh TRIM5α (Anderson et al., 2006; Wu et al., 2006). We therefore examined levels of late reverse transcribed products and 2-LTR forms of HIV-1 cDNA in TRIM5α-expressing cells by real time PCR method. Mean C_T values (SD) of late reverse transcribed products were 29.80 (0.27), 29.30 (0.15), and 28.11 (0.10) in cells expressing Rh, AGM, and Hu-R332P TRIM5αs, respectively, while that in control cells was 24.73 (0.08). These results clearly indicated that synthesis of late reverse transcribed products were suppressed in cells expressing functional TRIM5α. When we added MG132, mean C_T values (SD) of late reverse transcribed products were 29.16 (0.13), 28.72 (0.10), and 26.96 (0.15) in cells expressing Rh, AGM, and Hu-R332P TRIM5αs, respectively, and that in control cells was 24.63 (0.11). Differences between C_T values in the presence of MG132 and those in the absence of MG132 were statistically significant ($P<0.05$) in cells expressing Rh, AGM, and Hu-R332P TRIM5αs but not in control cells. We therefore concluded that slight but significant levels of late reverse transcribed products were recovered by MG132 treatment in cells expressing Rh, AGM, and Hu-R332P TRIM5αs. It should be noted that we failed to obtain complete recovery of late reverse transcribed products by MG132 treatment in our experimental system. This was most likely caused by incomplete suppression of proteasome function in our system since SeV-infected MT4 cells could be treated with MG132 for only 2 h to maintain cell viability, while Hela cells were treated with MG132 for 15 h in the previous studies (Anderson et al., 2006; Wu et al., 2006).

With respect to 2-LTR forms of HIV-1 cDNA, mean C_T values (SD) in the absence of MG132 were 39.99 (1.74), 38.32 (2.36), and 37.81 (1.80) in cells expressing Rh, AGM, and Hu-R332P TRIM5αs, respectively, and that in control cells was 33.68 (0.64). In the presence of MG132, mean C_T values (SD) were 40.02 (1.71), 38.71 (1.39), and 36.46 (2.03) in cells expressing Rh, AGM, and Hu-R332P TRIM5αs, respectively, and that in control cells was 33.80 (0.28). Significant recovery of 2-LTR forms of HIV-1 cDNA was thus observed only in cells expressing Hu-R332P TRIM5α ($P<0.05$) but not in cells expressing either AGM or Rh TRIM5αs. These results confirmed that HIV-1 restriction by Rh and AGM TRIM5αs was both proteasome dependent and independent while that by HuR332P TRIM5α was mainly proteasome dependent.

Discussion

Deletion of the RING domain or amino acid changes within the RING domain of Rh TRIM5α has been shown to attenuate anti-HIV-1 activity, but such a mutated TRIM5α still exhibits moderate HIV-1 restriction (Javanbakht et al., 2005; Perez-Caballero et al., 2005b; Stremlau et al., 2004). Both proteasome-dependent and -independent pathways have been proposed in HIV-1 restriction by Rh TRIM5α, since proteasome inhibitor MG132 allows HIV-1 to generate late reverse transcribed products, even though HIV-1 infection and the generation of nuclear 1-LTR and 2-LTR viral cDNA forms remain impaired by Rh TRIM5α (Anderson et al., 2006; Wu et al., 2006). In the study presented here, we demonstrated that the contribution of the RING domain of TRIM5α to retrovirus restriction differed among viral species. SIVmac completely escaped attacks by RING mutants of

Table 1
Summary of TRIM5α-mediated restriction.

	Anti-HIV-1 activity		Anti-SIVmac activity	
TRIM5α	proteasome-dependen	proteasome-independent	proteasome-dependen	proteasome-independent
AGM	yes	yes	yes	no
AGM C15AC18A	no	yes	no	no
AGM with MG132	no	yes	no	no
Hu R332P	yes	no	yes	no
Hu-R332P C15AC18A	no	no	no	no
Hu R332P with MG132	no	no	no	no

Yes, presence of the pathway;
no, absence of the pathway.

Please cite this article as: Maegawa, H., et al., Contribution of RING domain to retrovirus restriction by TRIM5α depends on combination of host and virus, Virology (2010), doi:10.1016/j.virol.2010.01.003

TRIM5α that could still moderately restrict HIV-1 and HIV-2 infection. Addition of proteasome inhibitor MG132 had no effect at all on the anti-HIV-1 activity of AGM TRIM5α, whereas it disrupted at least partly the anti-SIVmac activity of AGM TRIM5α. These results indicate that SIVmac is restricted by AGM TRIM5α mainly in a proteasome-dependent manner, whereas HIV-1 restriction by AGM, Rh, and cynomolgus monkey TRIM5α is both proteasome dependent and independent. In case of Hu-R332P TRIM5α, however, both HIV-1 and SIVmac restrictions were completely eliminated by mutations in the RING domain. Furthermore, both anti-HIV-1 and anti-SIVmac activities of Hu-R332P TRIM5α could also be disrupted by the proteasome inhibitor. These findings indicate that Hu-R332P TRIM5α restricts both HIV-1 and SIVmac mainly via the proteasome-dependent pathway.

It was found that TRIM5α could be poly-ubiquitinated and degraded by the proteasome (Diaz-Griffero et al., 2006). Furthermore, accelerated turnover of TRIM5α was observed during HIV-1 restriction (Rold and Aiken, 2008). Although there is no direct evidence for ubiquitination of the virus core by TRIM5α, it is highly likely that reverse transcription complexes containing viral CA proteins recognized by poly-ubiquitinated TRIM5α would be degraded by the proteasome in combination with TRIM5α. On the other hand, the exact molecular mechanism of the proteasome-independent pathway is still unclear at present. It was previously shown that the incubation of *in vitro* assembled CA proteins composed of recombinant HIV-1 CA–NC fusion proteins with the TRIM5-21R protein containing the Rh TRIM5α B-box, coiled-coil, and SPRY domains and the TRIM21 RING domain caused apparent breaks in the CA structure without any other cellular components (Langelier et al., 2008). It is thus likely that direct binding of Rh TRIM5α proteins to incoming HIV-1 CA proteins causes CA disassembly, which is observed as proteasome-independent restriction. AGM TRIM5α would bind both HIV-1 and SIVmac CA, while it may cause disassembly of the HIV-1 CA but not that of the SIVmac CA. Similarly, Hu-R332P TRIM5α would bind both HIV-1 and SIVmac CA but may fail to cause disassembly of both HIV-1 and SIVmac CAs. We therefore speculate that the proteasome-independent pathway requires specific SPRY–CA interaction that can lead to CA disassembly.

Although the proteasome inhibitor clearly disrupted anti-HIV-1 activity of Hu-R332P and anti-SIVmac activity of AGM, Hu-R332P, and human/AGM TRIM5αs, the number of infected cells never reached the levels of the negative control AGM-TRIM5α-CC(−). Longer exposure of cells expressing the TRIM5αs with the proteasome inhibitor did not increase the number of infected cells (data not shown). In contrast, anti-HIV-1 activity of Hu-R332P and anti-SIVmac activity of AGM and Hu-R332P TRIM5αs were completely eliminated by mutations in the RING domain. The reason for this discrepancy is not clear at present, but it is possible that TRIM5α also exerts a proteasome-independent but RING-dependent restrictive effect.

The RING-proteasome-independent restriction pathway was observed only in anti-HIV-1 but not in anti-SIVmac activity of AGM TRIM5α. It is known that cyclophilin A (CypA) binds to HIV-1 CA via the loop between the 4th and 5th α-helices (L4/5) but not to SIVmac CA (Luban et al., 1993). Since CypA was reported to restrict HIV-1 in monkey cells (Berthoux et al., 2005; Keckesova et al., 2006; Nakayama et al., 2008; Sokolskaja et al., 2006; Stremlau et al., 2006b), it is possible that CypA binding to HIV-1 CA regulates the RING-proteasome-independent restriction mechanism of TRIM5α (Berthoux et al., 2004). This hypothesis prompted us to examine the effect of the RING mutation of TRIM5α on its restrictive effect on NL-ScaVR, an HIV-1 derivative containing SIVmac L4/5 of CA and vif (Kamada et al., 2006). However, NL-ScaVR was similarly restricted by AGM TRIM5α with C15AC18A to HIV-1 (data not shown), indicating that neither the CypA-binding site nor vif is the determining factor in RING-proteasome-independent restriction of HIV-1. Further studies using various chimeric viruses between HIV-1 and SIVmac will also be needed to elucidate the exact molecular mechanisms of the RING-proteasome-independent pathway of TRIM5α mediated HIV-1 restriction.

Conclusion

AGM TRIM5α restricted SIVmac mainly via the proteasome-dependent pathway, whereas HIV-1 and HIV-2 restriction by AGM TRIM5α was both proteasome dependent and independent. In contrast, Hu-R332P restricts both HIV-1 and SIVmac mainly via the proteasome-dependent pathway. We concluded that the mechanisms of retrovirus restriction by TRIM5α vary depending on the combination of host and virus.

Materials and methods

Plasmid construction and protein expression

Previous reports have described recombinant Sendai viruses (SeVs) expressing C-terminally HA-tagged AGM TRIM5α (GenBank accession number AB210050), Rh TRIM5α (GenBank accession number AY625001), cynomolgus monkey (CM) TRIM5α (GenBank accession number AB210052), human TRIM5α (This human TRIM5α cDNA was obtained from T cell line MT4 and there was a single glycine-to-aspartic acid substitution at an amino acid position 249 compared with GenBank accession number NM033034.1), human TRIM5α with R332P, human and AGM chimeric TRIM5α and AGM TRIM5α lacking the coiled-coil domain (AGM-TRIM5α-CC(−)) (Kono et al., 2008; Maegawa et al., 2008; Nakayama et al., 2005, 2007). In the present study, a PCR-based mutagenesis was used to generate cDNA of the following C-terminally HA-tagged AGM TRIM5α RING domain mutants: AGM TRIM5α with C15AC18A, AGM TRIM5α with C30AH32A, AGM TRIM5α with C15AC18A-C30AH32A, and human TRIM5α with R332P and C15AC18A mutations. The entire coding sequences of those TRIM5αs were then transferred to the NotI site of pSeV18+b(+). Recombinant SeVs expressing various TRIM5αs were obtained with a previously described method (Shioda et al., 2001).

The plasmid expressing myc-tagged ubiquitin (myc-Ub) was generated according to the previous publication (Ellison and Hochstrasser, 1991). Briefly, human ubiquitin cDNA (NM_018955) was amplified by reverse transcription-PCR from the human epithelial carcinoma cell line HeLa by using 5′-GCGAATGCCATGACTGAAG-3′ and 5′-GACGTGGTTGGTGATTGGC-3′ followed by nested PCR using 5′-ATGCAGATCTTCGTGAAAACC-3′ and 5′-CTAACCACCTCTCAGACGCAG-GACC-3′. The amplified products were then cloned into pCR-2.1 TOPO (Invitrogen, Carlsbad, CA). The entire coding sequences of the myc-Ub were then transferred to the NheI and NotI site of pcDNA3.1(-) (Invitrogen, Carlsbad, CA).

Immunoprecipitation and Western blot analysis

For protein expression analysis, human T-cell line MT4 was infected with SeV at a multiplicity of infection (MOI) of 10 plaque forming units (PFU) per cell, and incubated at 37 °C for 16 h. The cells were then lysed in RIPA buffer (10 mM Tris–HCl (pH 7.4) containing 100 mM NaCl, 1% Sodium deoxycholate, and 0.1% sodium dodecyl sulfate), and the cell lysates were subjected to sodium dodecyl sulfate-polyacrylamide gel electrophoresis (SDS-PAGE). Proteins in the gel were transferred to a membrane (Immobilon; Millipore, Billerica, MA), and blots were blocked and probed with an anti-HA High Affinity rat monoclonal antibody (Roche, Indianapolis, IN) overnight at 4 °C. Blots were then incubated with peroxidase-conjugated anti-rat IgG (American Qualex, San Clemente, CA). Bound antibodies were visualized with ChemiLumi-One L chemiluminescent kit (Nacalai Tesque, Kyoto, Japan).

Please cite this article as: Maegawa, H., et al., Contribution of RING domain to retrovirus restriction by TRIM5α depends on combination of host and virus, Virology (2010), doi:10.1016/j.virol.2010.01.003

For ubiquitination analysis, the NotI and EcoRI sites were used to construct the plasmid expressing HA-tagged TRIM5α RING mutants in pcDNA3.1(-). DMRIE-C reagent (Invitrogen, Carlsbad, CA) was used to transfect 293 T cells with 1 μg of plasmid encoding HA-tagged wild-type or mutant TRIM5αs together with 1 μg of plasmid expressing myc-Ub in six-well plates. Forty-eight hours later, the cells were lysed and TRIM5α proteins in the lysates were precipitated with a Protein G-immunoprecipitation kit (Roche, Indianapolis, IN) using the anti-HA rat monoclonal antibody. After overnight incubation at 4 °C, beads were washed three times in RIPA buffer. Precipitated proteins were detected with the same procedure as above except that an anti-myc mouse monoclonal antibody and peroxidase-conjugated anti-mouse IgG (Kirkegaard and Perry Laboratories, Gaithersburg, MD) were used for visualizing the myc-tagged Ub protein.

Virus preparation

HIV-1-NL43, HIV-2 GH123 or SIVmac239 was prepared by transfection of 293 T cells with pNL432 (Adachi et al., 1986), pGH123 (Shibata et al., 1990), or pBRmac239 (Kastler et al., 1991), respectively. The vesicular stomatitis virus glycoprotein (VSV-G) pseudotyped HIV-1 vector expressing green fluorescence protein (GFP) (HIV-1-GFP) was prepared as described previously (Miyoshi et al., 1997, 1998) as was VSV-G pseudotyped SIVmac vector expressing GFP (SIVmac-GFP) (Hofmann et al., 1999). The viral titer was determined by measuring viral CA protein, p24, p25 or p27, with a RetroTek antigen ELISA kit (ZeptoMetrix, Buffalo, NY).

Viral infection

MT4 or canine Cf2Th cells were infected with SeV expressing various TRIM5αs. Nine hours after SeV infection, 1.0×10^5 cells per dose were superinfected with serially diluted HIV-1-GFPs or SIVmac-GFPs in 48-well plates and incubated at 37 °C. Forty hours after infection, the infected cells were fixed with 1% formaldehyde and counted with a flow cytometer (FACScaliber; Becton Dickinson, Franklin Lakes, NJ). For the HIV-1, HIV-2 or SIVmac replication assay, 2.0×10^5 MT4 cells were infected with SeV expressing various TRIM5αs and 9 h after SeV infection, the cells were superinfected with 20 ng of p24 of HIV-1 NL43, p25 of HIV-2 GH123 or p27 of SIVmac. The culture supernatants were collected periodically for measurement of the p24, p25 or p27 levels.

Proteasome inhibition and infection with HIV-1-GFP or SIVmac-GFP

MT4 cells were infected with SeV expressing various TRIM5αs. Nine hours after SeV infection, 1.0×10^5 cells were superinfected with 10 ng of p24 of HIV-1-GFP or 100 ng of p27 of SIVmac-GFP in the presence of 10 μM MG132 (CALBIOCHEM) in 0.1% DMSO or 0.1% DMSO only. Two hours after the HIV-1-GFP or SIVmac-GFP infection, the cells were washed in fresh medium and incubated at 37 °C for 40 h. The infected cells were fixed with 1% formaldehyde and then counted with a flow cytometer.

Immunofluorescence confocal microscopy

AGM CV1 cells infected with SeV expressing several TRIM5αs at an MOI of 10 PFU per cell were fixed 24 h after infection in 3% paraformaldehyde in PBS, permeabilized with 0.05% saponin and 0.2% bovine serum albumin in PBS, and incubated with the anti-HA rat monoclonal antibody. Bound antibodies were then detected with a FITC-conjugated goat antibody directed against rat IgG (American Qualex Antibodies, San Clemente, CA). Indirect immunofluorescence was visualized with a Radiance 2000 laser confocal microscope system (Bio-Rad Laboratories, Hercules, CA).

Real-time PCR analysis

To prepare high titer virus stock of HIV-1 NL43, MT4 cells were infected with NL43 virus and the culture supernatant was harvested at its peak titer (1250 ng/ml of p24) at 12 days after infection. Five x 10^6 MT4 cells were infected with SeV expressing TRIM5α. Twenty hours after SeV infection, cells were superinfected with 500 μl (625 ng of p24) of NL43 stock virus with 10 μM MG132 (CALBIOCHEM) in 0.1% DMSO or with 0.1% DMSO only for 2 h. After washing out of inoculated virus containing MG132, cells were suspended in 10 ml of flesh media and incubated at 37 C for 12 h. Total DNA was extracted by using QIAamp DNA Blood kit. Real-time PCR was performed with an Applied Biosystems 7500 Real-Time PCR System to analyze viral cDNA synthesis. Primers and Taqman probes for late reverse transcribed products and 2-LTR forms were designed according to Julias et al. (2001) and Van Maele et al. (2003), and 0.6 μg DNA were subjected to 40 cycles of PCR in 10 μl reaction mixture. Threshold cycle (C_T) values were calculated by 7500 Fast System SDS software (Applied Biosystems). Mean C_T values and their standard deviation (SD) were calculated in triplicate (late reverse transcribed product) or septuplicate (2-LTR) samples. In a few cases we failed to detect amplification of 2-LTR forms, the C_T values were assigned as 41 cycles. Statistical significance of observed difference in mean C_T values was evaluated by Mann-Whitney U test.

Uncited references

Q2

Berthous et al., 2004
Kestler et al., 1991

Acknowledgements

We are grateful to J. Sodroski and F. Diaz-Griffero (Harvard Medical School, Boston, USA) for providing the pSIvec1.GFP plasmid. We also wish to thank S. Sakuragi for her helpful discussions and S. Bando and N. Teramoto for their assistance. This work was supported by grants from the Ministry of Education, Culture, Sports, Science, and Technology, the Ministry of Health, Labor and Welfare, and the Health Science Foundation of Japan.

References

Abe, H., Miyamoto, K., Tochio, N., Koshiba, S., Kigawa, T., Yokoyama, S., 2007. Solution structure of the zinc finger, C3hc4 type (ring finger) domain of tripartite motif-containing protein 5. MMDB: Entrez's 3D-structure database. MMDB ID: 62462. http://www.ncbi.nlm.nih.gov/Structure/mmdb/mmdbsrv.cgi?Dopt = s&uid = 62462

Adachi, A., Gendelman, H.E., Koeing, S., Folks, T., Willey, R., Rabson, A., Martin, M.A., 1986. Production of acquired immunodeficiency syndrome associated retrovirus in human and nonhuman cells transfected with an infectious molecular clone. J. Virol. 59, 284–291.

Anderson, J.L., Campbell, E.M., Wu, X., Vandegraaff, N., Engelman, A., Hope, T.J., 2006. Proteasome inhibition reveals that a functional preintegration complex intermediate can be generated during restriction by diverse TRIM5 proteins. J. Virol. 80, 9754–9760.

Berthous, L., Sebastian, S., Sokolskaja, E., Luban, J., 2004. Lv1 inhibition of human immunodeficiency virus type 1 is counteracted by factors that stimulate synthesis or nuclear translocation of viral cDNA. J. Virol. 78, 11359–11739.

Berthoux, L., Sebastian, S., Sokolskaja, E., Luban, J., 2005. Cyclophilin A is required for TRIM5α-mediated resistance to HIV-1 in Old World monkey cells. Proc. Natl. Acad. Sci. U.S.A. 102, 14849–14853.

Borden, K.L., Boddy, M.N., Lally, J., O'Reilly, N.J., Martin, S., Howe, K., Solomon, E., Freemont, P.S., 1995. The solution structure of the RING finger domain from the acute promyelocytic leukaemia proto-oncoprotein PML. EMBO J. 14, 1532–1541.

Borden, K.L., Freemont, P.S., 1996. The RING domain: a recent example of a sequence-structure family. Curr. Opin. Struct. Biol. 1996 (6), 395–401.

Diaz-Griffero, F., Li, X., Javanbakht, H., Song, B., Welikala, S., Stremlau, M., Sodroski, J., 2006. Rapid turnover and polyubiquitylation of the retroviral restriction factor TRIM5. Virology 349, 300–315.

Ellison, M.J., Hochstrasser, M., 1991. Epitope-tagged ubiquitin. A new probe for analyzing ubiquitin function. J. Biol. Chem. 266, 21150–21157.

Gao, F., Bailes, E., Robertson, D.L., Chen, Y., Rodenburg, C.M., Michael, S.F., Cummins, L.B., Arthur, L.O., Peeters, M., Shaw, G.M., Sharp, P.M., Hahn, B.H., 1999. Origin of HIV-1 in the chimpanzee Pan troglodytes troglodytes. Nature 397, 436–441.

Please cite this article as: Maegawa, H., et al., Contribution of RING domain to retrovirus restriction by TRIM5α depends on combination of host and virus, Virology (2010), doi:10.1016/j.virol.2010.01.003

Hofmann, W., Schubert, D., LaBonte, J., Munson, L., Gibson, S., Scammell, J., Ferrigno, P., Sodroski, J., 1999. Species-specific, postentry barriers to primate immunodeficiency virus infection. J. Virol. 73, 10020–10028.

Jackson, P.K., Eldridge, A.G., Freed, E., Furstenthal, L., Hsu, J.Y., Kaiser, B.K., Reimann, J.D., 2000. The role of the RINGs: substrate recognition and catalysis by ubiquitin ligases. Trends Cell Biol. 10, 429–439.

Javanbakht, H., Diaz-Griffero, F., Stremlau, M., Si, Z., Sodroski, J., 2005. The contribution of RING and B-box 2 domains to retrovirus restriction mediated by monkey TRIM5α. J. Biol. Chem. 280, 26933–26940.

Javanbakht, H., Yuan, W., Yeung, D.F., Song, B., Diaz-Griffero, F., Li, Y., Li, X., Stremlau, M., Sodroski, J., 2006. Characterization of TRIM5α trimerization and its contribution to human immunodeficiency virus capsid binding. Virology 353, 234–246.

Julias, J.G., Ferris, A.L., Boyer, P.L., Hughes, S.H., 2001. Replication of phenotypically mixed human immunodeficiency virus type 1 virions containing catalytically active and catalytically inactive reverse transcriptase. J. Virol. 6537–6546.

Kamada, K., Igarashi, T., Martin, M.A., Khamsri, B., Hatcho, K., Yamashita, T., Fujita, M., Uchiyama, T., Adachi, A., 2006. Generation of HIV-1 derivatives that productively infect macaque monkey lymphoid cells. Proc. Natl. Acad. Sci. U.S.A. 103, 16959–16964.

Keckesova, Z., Ylinen, L.M., Towers, G.J., 2006. Cyclophilin A renders human immunodeficiency virus type 1 sensitive to old world monkey but not human TRIM5α antiviral activity. J. Virol. 80, 4683–4690.

Kestler III, H.W., Ringler, D.J., Mori, K., Panicali, D.L., Sehgal, P.K., Daniel, M.D., Desrosiers, R.C., 1991. Importance of the nef gene for maintenance of high virus loads and for development of AIDS. Cell 65, 651–662.

Kono, K., Song, H., Shingai, Y., Shioda, T., Nakayama, E.E., 2008. Comparison of anti-viral activity of rhesus monkey and cynomolgus monkey TRIM5αs against HIV-2 infection. Virology 373, 447–456.

Langelier, C.R., Sandrin, V., Eckert, D.M., Christensen, D.E., Chandrasekaran, V., Alam, S.L., Aiken, C., Olsen, J.C., Kar, A.K., Sodroski, J.G., Sundquist, W.I., 2008. Biochemical characterization of a recombinant TRIM5α protein that restricts human immunodeficiency virus type 1 replication. J. Virol. 82, 11682–11694.

Luban, J., Bossolt, K.L., Franke, E.K., Kalpana, G.V., Goff, S.P., 1993. Human immunodeficiency virus type 1 Gag protein binds to cyclophilins A and B. Cell 73, 1067–1078.

Maegawa, H., Nakayama, E.E., Kuroishi, A., Shioda, T., 2008. Silencing of tripartite motif protein (TRIM) 5α mediated anti-HIV-1 activity by truncated mutant of TRIM5α. J. Virol. Methods 151, 249–256.

Mische, C.C., Javanbakht, H., Song, B., Diaz-Griffero, F., Stremlau, M., Strack, B., Si, Z., Sodroski, J., 2005. Retroviral restriction factor TRIM5α is a trimer. J. Virol. 79, 14446–14450.

Miyoshi, H., Takahashi, M., Gage, F.H., Verma, I.M., 1997. Stable and efficient gene transfer into the retina using an HIV-based lentiviral vector. Proc. Natl. Acad. Sci. U.S.A. 94, 10319–10323.

Miyoshi, H., Blomer, U., Takahashi, M., Gage, F.H., Verma, I.M., 1998. Development of a self-inactivating lentivirus vector. J. Virol. 72, 8150–8157.

Nakayama, E.E., Miyoshi, H., Nagai, Y., Shioda, T., 2005. A specific region of 37 amino acid residues in the SPRY (B30.2) domain of African green monkey TRIM5α determines species-specific restriction of simian immunodeficiency virus SIVmac infection. J. Virol. 79, 8870–8877.

Nakayama, E.E., Carpentier, W., Costagliola, D., Shioda, T., Iwamoto, A., Debre, P., Yoshimura, K., Autran, B., Matsushita, S., Theodorou, I., 2007. Wild type and H43Y variant of human TRIM5α show similar anti-human immunodeficiency virus type 1 activity both in vivo and in vitro. Immunogenetics 59, 511–515.

Nakayama, E.E., Shingai, Y., Kono, K., Shioda, T., 2008. TRIM5α-independent anti-human immunodeficiency virus type 1 activity mediated by cyclophilin A in Old World monkey cells. Virology 375, 514–520.

Perez-Caballero, D., Hatziioannou, T., Yang, A., Cowan, S., Bieniarz, P.D., 2005a. Human tripartite motif 5α domains responsible for retrovirus restriction activity and specificity. J. Virol. 79, 8969–8978.

Perez-Caballero, D., Hatziioannou, T., Zhang, F., Cowan, S., Bieniasz, P.D., 2005b. Restriction of human immunodeficiency virus type 1 by TRIM-CypA occurs with rapid kinetics and independently of cytoplasmic bodies, ubiquitin, and proteasome activity. J. Virol. 79, 15567–15572.

Reymond, A., Meroni, G., Fantozzi, A., Merla, G., Cairo, S., Luzi, L., Riganelli, D., Zanaria, E., Messali, S., Cainarca, S., Guffanti, A., Minucci, S., Pelicci, P.G., Ballabio, A, 2001. The tripartite motif family identifies cell compartments. EMBO J. 20, 2140–2151.

Rold, C.J., Aiken, C., 2008. Proteasomal degradation of TRIM5α during retrovirus restriction. PLoS. Pathog. 4, 5.

Sawyer, S.L., Wu, L.I., Emerman, M., Malik, H.S., 2005. Positive selection of primate TRIM5α identifies a critical species-specific retrovirus restriction domain. Proc. Natl. Acad. Sci. U.S.A. 102, 2832–2837.

Sawyer, S.L., Emerman, M., Malik, H.S., 2007. Discordant evolution of the adjacent antiretroviral genes *TRIM22* and *TRIM5* in mammals. PloS Pathog. 3, 1918–1929.

Sebastian, S., Luban, J., 2005. TRIM5alpha selectively binds a restriction-sensitive retroviral capsid. Retrovirology 2, 40.

Shibata, R., Miura, T., Hayami, M., Ogawa, K., Sakai, H., Kiyomasu, T., Ishimoto, A., Adachi, A., 1990. Mutational analysis of the human immunodeficiency virus type 2 (HIV-2) genome in relation to HIV-1 and simian immunodeficiency virus SIV (AGM). J. Virol. 64, 742–747.

Shioda, T., Nakayama, E.E., Tanaka, Y., Xin, X., Liu, H., Kawana-Tachikawa, A., Kato, A., Sakai, Y., Nagai, Y., Iwamoto, A., 2001. Naturally occurring deletional mutation in the C-terminal cytoplasmic tail of CCR5 affects surface trafficking of CCR5. J. Virol. 75, 3462–3468.

Sokolskaja, E., Berthoux, L., Luban, J., 2006. Cyclophilin A and TRIM5α independently regulate human immunodeficiency virus type 1 infectivity in human cells. J. Virol. 80, 2855–2862.

Song, B., Javanbakht, H., Perron, M., Park, D.H., Stremlau, M., Sodroski, J., 2005. Retrovirus restriction by TRIM5α variants from Old World and New World Primates. J. Virol. 79, 3930–3937.

Stremlau, M., Owens, C.M., Perron, M.J., Kiessling, M., Autissier, P., Sodroski, J., 2004. The cytoplasmic body component TRIM5α restricts HIV-1 infection in Old World monkeys. Nature 427, 848–853.

Stremlau, M., Perron, M., Welikala, S., Sodroski, J., 2005. Species-specific variation in the B30.2 (SPRY) domain of TRIM5α determines the potency of human immunodeficiency virus restriction. J. Virol. 79, 3139–3145.

Stremlau, M., Perron, M., Lee, M., Li, Y., Song, B., Javanbakht, H., Diaz-Griffero, F., Anderson, D.J., Sundquist, W.I., Sodroski, J., 2006a. Specific recognition and accelerated uncoating of retroviral capsids by the TRIM5α restriction factor. Proc. Natl. Acad. Sci. U.S.A. 103, 5514–5519.

Stremlau, M., Song, B., Javanbakht, H., Perron, M., Sodroski, J., 2006b. Cyclophilin A: an auxiliary but not necessary cofactor for TRIM5α restriction of HIV-1. Virology 351, 112–120.

Van Maele, B., Rijck, J.D., Clercq, E.D., Debyser, Z., 2003. Impact of the central polypurine tract on the kinetics of human immunodeficiency virus type 1 vector transduction. J. Virol. 4685–4694.

Wu, X., Anderson, J.L., Campbell, E.M., Joseph, A.M., Hope, T.J., 2006. Proteasome inhibitors uncouple rhesus TRIM5α restriction of HIV-1 reverse transcription and infection. Proc. Natl. Acad. Sci. U.S.A. 103, 7465–7470.

Yap, M.W., Nisole, S., Stoye, J.P., 2005. A single amino acid change in the SPRY domain of human TRIM5α leads to HIV-1 restriction. Curr. Biol. 15, 73–78.

Please cite this article as: Maegawa, H., et al., Contribution of RING domain to retrovirus restriction by TRIM5α depends on combination of host and virus, Virology (2010), doi:10.1016/j.virol.2010.01.003

Bioorganic & Medicinal Chemistry Letters 20 (2010) 354–358

Contents lists available at ScienceDirect

Bioorganic & Medicinal Chemistry Letters

journal homepage: www.elsevier.com/locate/bmcl

CD4 mimics targeting the mechanism of HIV entry

Yuko Yamada [a], Chihiro Ochiai [a], Kazuhisa Yoshimura [b], Tomohiro Tanaka [a], Nami Ohashi [a], Tetsuo Narumi [a], Wataru Nomura [a], Shigeyoshi Harada [b], Shuzo Matsushita [b], Hirokazu Tamamura [a,*]

[a] Institute of Biomaterials and Bioengineering, Tokyo Medical and Dental University, Chiyoda-ku, Tokyo 101-0062, Japan
[b] Center for AIDS Research, Kumamoto University, Kumamoto 860-0811, Japan

ARTICLE INFO

Article history:
Received 19 September 2009
Revised 20 October 2009
Accepted 22 October 2009
Available online 4 November 2009

Keywords:
CD4 mimic
HIV entry
Synergistic effect
CXCR4

ABSTRACT

A structure–activity relationship study was conducted of several CD4 mimicking small molecules which block the interaction between HIV-1 gp120 and CD4. These CD4 mimics induce a conformational change in gp120, exposing its co-receptor-binding site. This induces a highly synergistic interaction in the use in combination with a co-receptor CXCR4 antagonist and reveals a pronounced effect on the dynamic supramolecular mechanism of HIV-1 entry.

Recently, remarkable success has attended the clinical treatment of HIV-infected and AIDS patients, with 'highly active antiretroviral therapy (HAART)'. This approach involves a combination of two or three agents from two categories: reverse transcriptase inhibitors and protease inhibitors.[1] In addition, the molecular mechanism involved in HIV-entry and -fusion into host cells has been described in detail.[2] The complex interactions of surface proteins on cellular and viral membranes, which are designated as a dynamic supramolecular mechanism of HIV entry, are reported to be crucial to the viral infection. In a first step, an HIV envelope protein, gp120 interacts with a cell surface protein, CD4, leading to a conformational change in gp120 followed by subsequent binding of gp120 to a co-receptor CCR5[3] or CXCR4.[4] CCR5 and CXCR4 are the major co-receptors for the entry of macrophage-tropic (R5-) and T cell line-tropic (X4-) HIV-1, respectively. The interaction of gp120 with CCR5 or CXCR4 triggers entry of another envelope protein, gp41 to the cell membrane and formation of a gp41 trimer-of-hairpins structure, which causes fusion of HIV/cell-membranes and completes the infection.

Informed by this mechanism, a fusion inhibitor, enfuvirtide (fuzeon, Trimers & Roche)[5] and a CCR5 antagonist, maraviroc (Pfizer)[6] in addition to an integrase inhibitor, raltegravir (Merck)[7] have been used clinically. However, serious problems with chemotherapy still persist, including the emergence of viral strains with multi-drug resistance (MDR), considerable adverse effects and high costs. Consequently, development of novel drugs possessing mechanisms of action different from those of the above inhibitors is currently required. We have previously developed selective CXCR4 antagonists[8] and fusion inhibitors.[9] Furthermore, *N*-(4-Bromophenyl)-*N'*-(2,2,6,6-tetramethylpiperidin-4-yl)-oxalamide (**1**) and *N*-(4-chlorophenyl)-*N'*-(2,2,6,6-tetramethylpiperidin-4-yl)-oxalamide (**2**) were previously found using chemical library screening to inhibit syncytium formation by other researchers.[10] **1** and **2** bind to gp120 with binding affinities of K_d = 2.2 μM and 3.7 μM, respectively, blocking the interaction of gp120 with CD4 in the first step of an HIV-1 entry. Thus, in the present study we focus on the development of CD4 mimics that can block the interaction between gp120 and CD4. We have investigated the effect of CD4 mimics on conformational changes of gp120 and on their use in combination use with a CXCR4 antagonist.

Initially, molecular modeling of compound **2** docked into gp120 was carried out using docking simulations performed by the FlexSIS module of SYBYL 7.1 (Tripos, St. Louis) (Fig. 1).[11] The atomic coordinates of the crystal structure of gp120 with soluble CD4 (sCD4) were retrieved from Protein Data Bank (PDB) (entry 1RZJ) (Fig. 1a) and it was observed that Phe^{43} and Arg^{59} of the CD4 have multiple contacts with Asp^{368}, Glu^{370} and Trp^{427} of gp120, which are all conserved residues. An inspection of the environment of compound **2** docked in gp120 revealed the presence of a large cavity around the *p*-position of the phenyl ring of compound **2**, which could interact with the viral surface protein gp120 (Fig. 1b and c). Several analogs of **2** with substituents on the phenyl ring were therefore synthesized.

All compounds except **12** were synthesized by previously published methods (Scheme 1).[10b,12,13] Aniline derivatives (**3**) were coupled with ethyl oxalyl chloride to yield the corresponding ethyl oxalamates **4**. Saponification of the above oxalamates to the corresponding free acids and the subsequent coupling with 4-ami-

* Corresponding author.
E-mail address: tamamura.mr@tmd.ac.jp (H. Tamamura).

0960-894X/$ - see front matter © 2009 Elsevier Ltd. All rights reserved.
doi:10.1016/j.bmcl.2009.10.098

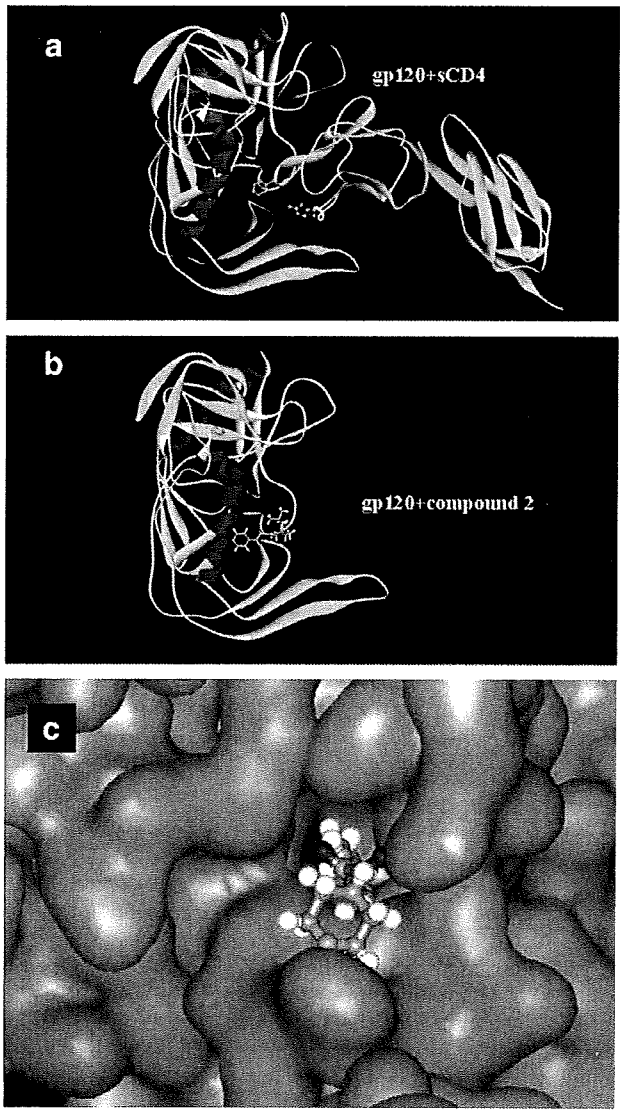

Figure 1. (a) The crystal structure of gp120 with soluble CD4 (sCD4) retrieved from the PDB (entry 1RZJ); (b) docking structure of compound **2** and gp120; (c) a focused figure of (b) shown by space-filling model.

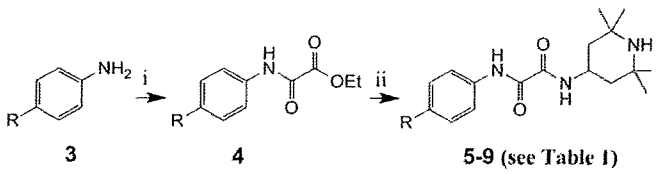

Scheme 1. Reagents and conditions: (i) ethyl oxalyl chloride, Et_3N; (ii) 1 M NaOH; 4-amino-2,2,6,6-tetramethylpiperidine, 1-(3-dimethylaminopropyl)-3-ethylcarbodiimide hydrochloride, 1-hydroxybenzotriazole, Et_3N.

no-2,2,6,6-tetramethylpiperidine using 1-ethyl-3-(3-dimethylaminopropyl)carbodiimide hydrochloride (EDC) and 1-hydroxybenzotriazole (HOBt) yielded compounds **5–9**. In the case of compound **12**, whose amide bond is not stable during the reaction of the saponification of the corresponding oxalamates, an alternative synthetic scheme was used (Scheme 2).[14] The reaction of *p*-nitroaniline (**10**) with oxalyl chloride gave the corresponding oxoacetamide **11**, which was subsequently coupled with 4-amino-2,2,6,6-tetramethylpiperidine to yield the desired compound **12**.

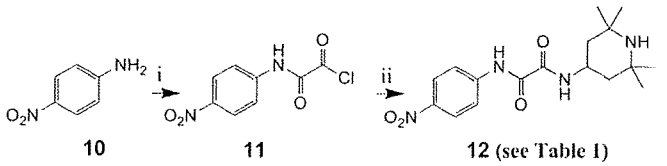

Scheme 2. Reagents and conditions: (i) oxalyl chloride, Et_3N; (ii) 4-amino-2,2,6,6-tetramethylpiperidine, Et_3N.

The anti-HIV activity of the synthetic compounds was evaluated against various viral strains including both laboratory and primary isolates (Table 1). IC_{50} values were determined by the 3-(4,5-dimethylthiazol-2-yl)-2,5-diphenyltetrazolium bromide (MTT) method[15] as the concentrations of the compounds which conferred 50% protection against HIV-1-induced cytopathogenicity in PM1/CCR5 cells. Cytotoxicity of the compounds based on the viability of mock-infected PM1/CCR5 cells was also evaluated using the MTT method. CC_{50} values were determined as the concentrations achieving 50% reduction of the viability of mock-infected cells. Compounds **1** and **2** showed potent anti-HIV activity against laboratory isolates, IIIB (X4, Sub B) and 89.6 (dual, Sub B) strains, and compound **2** also possessed potent activity against a primary isolate, an fTOI strain (R5, Sub B). All of the IC_{50} values were between 4 μM and 10 μM. Compound **1** was not tested against primary isolates. The potencies of compounds **1** and **2** are comparable to the reported binding affinities for gp120 (K_d = 2.2 and 3.7 μM, respectively).[10] Several of the new analogs of compounds **1** and **2** showed significant anti-HIV activity. Compound **5**, which has a phenyl group in place of the *p*-chlorophenyl group of compound **2**, did not show significant anti-HIV activity at concentrations below 100 μM against all strains tested except for an fTOI strain (R5, Sub B). This result suggests that a substituent at the *p*-position of the phenyl ring is critical for potent activity. Compound **6**, which has a fluorine atom at the *p*-position of the phenyl ring, showed moderate anti-HIV activity against laboratory isolates, IIIB (X4, Sub B) and 89.6 (dual, Sub B) strains (IC_{50} = 61 and 81 μM, respectively), but, at concentrations below 100 μM, failed to show significant anti-HIV activity against a primary isolate, a KYAG strain (R5, Sub B). Among halogen atoms, fluorine is less suitable than bromine or chlorine as a substituent at the *p*-position of the phenyl ring, as evidenced by compound **6**, which is 8–15-fold less potent than compounds **1** and **2** against IIIB (X4, Sub B) and 89.6 (dual, Sub B) strains. Compound **7**, which has a methyl group at the *p*-position of the phenyl ring, showed relatively more potent activity against IIIB (X4, Sub B) and 89.6 (dual, Sub B) strains (IC_{50} = 23 and 41 μM, respectively) than compound **6**. Compound **7** also showed significant anti-HIV activity against primary isolates, fTOI (R5, Sub B) and KYAG (R5, Sub B) strains (IC_{50} = 16 and 51 μM, respectively). Compound **8**, with a methoxy group at the *p*-position of the phenyl ring, did not show significant anti-HIV activity against all strains tested until a concentration of 100 μM was reached. In the biological assays, derivatives having electron-withdrawing substituents such as bromine, chlorine and fluorine at the *p*-position of the phenyl ring are relatively potent, whereas derivatives having electron-donating groups such as methoxy at this position are not potent. Furthermore, the steric effect of a substituent at the *p*-position of the phenyl ring appears to be critical to anti-HIV activity. The sum of Hammett constants (σ) of benzoic acid substituents[16] shown in Table 1 can be used to evaluate the electron-withdrawing or -donating effect of the substituents on the aromatic ring. The Taft E_s values[16a,17] were used as steric parameters for substituents at the *p*-position of the phenyl ring. The order of potency found for the halogen-containing derivatives in anti-HIV activity against laboratory isolates, IIIB (X4, Sub B) and 89.6 (dual, Sub B), is: compound **1** (R = Br) (σ = 0.23, E_s = −1.16), **2**

Table 1
Hammett constants (σ) and steric effects (E_s) of substituted aromatic rings and anti-HIV activity and cytotoxicity of synthetic compounds

Compd	R[a]	σ[b]	E_s[c]	IC_{50}[e] (μM)				CC_{50}[e] (μM)
				Lab. isolates		Primary isolates		
				IIIB (X4)	89.6 (dual)	fTOI (R5)	KYAG (R5)	
1	Br	0.23	−1.16	4	9	ND	ND	150
2	Cl	0.23	−0.97	8	10	5	>30	170
5	H	0	0	>100	>100	81	>100	350
6	F	0.06	−0.46	61	81	ND	>100	320
7	CH_3	−0.17	−1.24	23	41	16	51	210
8	OCH_3	−0.27	−0.55	>100	>100	ND	>100	340
9	CF_3	0.54	−2.40	ND	27	ND	ND	72
12	NO_2	0.78	−1.77[d]	ND	42	ND	ND	230
sCD4				0.010	0.021	0.0044	ND	ND

[a] See Schemes 1 and 2.
[b] σ = Hammett constant of a substitutent on a benzoic acid derivative.[16]
[c] E_s = steric effect of a substituent at the *para* position on the aromatic ring.[16a,17]
[d] The average value of −1.01 and −2.52, which are E_s values of the NO_2 group, −1.77, was used.
[e] Values are means of at least three experiments (ND = not determined).

(R = Cl) (σ = 0.23, E_s = −0.97), **6** (R = F) (σ = 0.06, E_s = −0.46) and **5** (R = H) (σ = 0, E_s = 0). This is the order of substituents' electron-withdrawing ability and also of their size. Methyl (σ = −0.17, E_s = −1.24) is an electron-donating group, but is almost as bulky as a bromine atom. Thus, the *p*-methyl derivative **7** has relatively potent anti-HIV activity against laboratory isolates, IIIB (X4, Sub B) and 89.6 (dual, Sub B), higher than that of compound **6** (R = F) but lower than that of compound **1** (R = Br) or **2** (R = Cl). The electron-donating ability of a methoxy group is stronger (σ = −0.27), but the bulk size is smaller (E_s = −0.55), than that of a methyl group. Thus, the *p*-methoxy derivative **8** has no significant anti-HIV activity against all strains tested at concentrations below 100 μM. Two derivatives containing bulkier and more potent electron-withdrawing substituents such as trifluoromethyl (R = CF_3) (σ = 0.54, E_s = −2.40) and nitro (R = NO_2) (σ = 0.78, E_s = −1.77) at the *p*-position of the phenyl ring were evaluated. Compounds **9** (R = CF_3) and **12** (R = NO_2) showed significant anti-HIV activity against an 89.6 (dual, Sub B) strain. These are less potent than compounds **1** and **2** and this is perhaps due to the excessive size of the substituents at the *p*-position. This suggests that a certain level of the bulk size and a potent electron-withdrawing ability of the substituents are preferable for anti-HIV activity. It is estimated that a cavity around the *p*-position of the phenyl ring of CD4 mimicking compounds would be optimally filled by bromine (E_s = −1.16) or a methyl group (E_s = −1.24) at *p*-position, and that an electron-deficient aromatic ring might interact tightly with a negatively charged group such as carboxy of Glu^{370}. In isothermal titration calorimetry (ITC) experiments reported elsewhere,[10c] compound **5** (R = H) does not have significant affinity for gp120, and compound **6** (R = F) has less potent affinity for gp120 than compound **2**, consistent with the present data. In all but one of the compounds, no significant cytotoxicity was detected (CC_{50} >150 μM, Table 1), the exception being compound **9** (R = CF_3) (CC_{50} = 72 μM). Compounds **7** and **12** have relatively low cytotoxicities, compared to compounds **1** and **2**.

Fluorescence activated cell sorting (FACS) analysis was performed[15] to investigate whether these synthetic compounds interact with gp120 inducing the conformational change necessary for the approach of an anti-envelope antibody or a co-receptor to the gp120. The profile of binding of an anti-envelope CD4-induced monoclonal antibody, 4C11, to the Env-expressing cell surface (an R5-HIV-1 strain, JR-FL,-infected PM1 cells) pretreated with the above CD4 mimic analogs was examined. Comparison of the binding of 4C11 to the cell surface was measured in terms of the mean fluorescence intensity (MFI), and is shown in Figure 2. Pretreatment of the Env-expressing cells with compound **2** (MFI = 38.42) produced a remarkable increase in binding affinity for 4C11, similar to that observed in pretreatment with sCD4 (MFI = 37.90). This is consistent with the results in the previous paper[10] where it was reported that compound **2** enhances the binding of gp120 to the 17b monoclonal antibody which recognizes the co-receptor binding site of gp120. Env-expressing cells, which were not pretreated with sCD4 or a CD4 mimic compound, did not show significant binding affinity for 4C11 (Fig. 2, blank). The increase in binding affinity for monoclonal antibodies may be due to conformational changes in gp120, which were caused by the interaction of sCD4 or a CD4 mimic with gp120. It is hypothesized that such conformational changes involve the exposure of the co-receptor binding site of gp120 (the V3 loop), which is hidden internally, since the binding of gp120 to 17b is enhanced. Compound **5**, which failed to show significant anti-HIV activity, and compounds **7**, **9** and **12**, which had significant anti-HIV activity, were assessed in the FACS analysis. The profile of the binding of 4C11 to the Env-expressing cell surface pretreated with compound **5** (MFI = 14.34) was similar to that of the blank (MFI = 11.24), suggesting that compound **5** offers no significant enhancement of binding affinity for 4C11. This result is compatible with the anti-HIV activity of compound **5**. The profile of the binding of 4C11 to the Env-expressing cell surface pretreated with compound **7** (MFI = 38.33) was entirely similar to that of compound **2** used as a pretreatment. Pretreatment of the cell surface with compounds **9** and **12** (MFI = 29.09 and 30.01, respectively) produced a slightly lower enhancement of binding affinity for 4C11, compared to those of compounds **2** and **7** as pretreatments. However, in the ITC experiments reported elsewhere,[10c] compound **9** (R = CF_3) has a high affinity for gp120, comparable to that of compound **2**, but compound **12** (R = NO_2) does not have significant affinity for gp120, indicating that these are not consistent with the current FACS studies, possibly due to the difference in the assay systems. Although the anti-HIV activity of **7** is weaker than that of compound **2**, the level of compound **7** inducing an enhancement of binding affinity of gp120 for 4C11 is comparable to that of compound **2**. The concentration of compounds used in the FACS analysis was 100 μM, much beyond the IC_{50} values of compounds **2** and **7**. A concentration of 100 μM would be also sufficient for the expression of anti-HIV activity caused by compounds **2** and **7**.

An effect on the use of compound **2** combined with another entry inhibitor was investigated. Analysis of the synergistic effects of anti-HIV agents was performed according to the median effect principle using the CalcuSyn version 2 computer program[18] to estimate IC_{50} values of compounds in different combinations. Combination indices (CI) were estimated from the data evaluated using the MTT assay

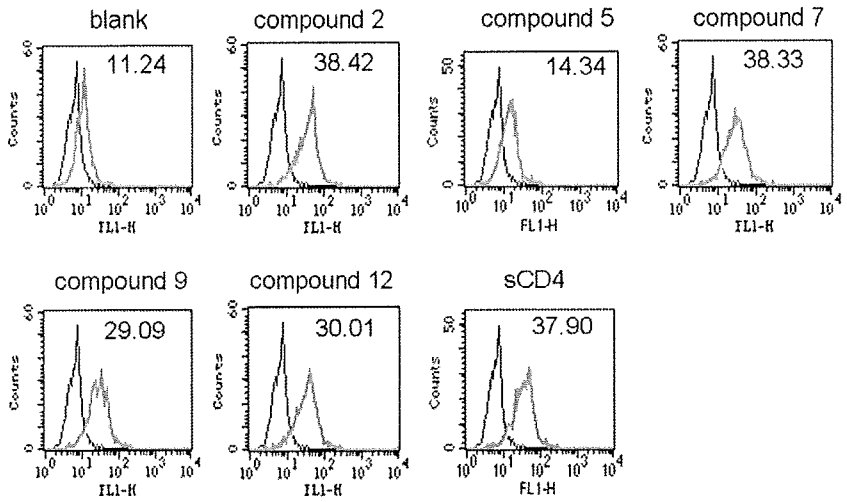

Figure 2. JR-FL (R5, Sub B) chronically infected PM1 cells were preincubated with 100 μM of a CD4 mimic or sCD4 (11 nM) for 15 min, and then incubated with an anti-HIV-1 mAb, 4C11, at 4 °C for 15 min. The cells were washed with PBS, and fluorescein isothiocyanate (FITC)-conjugated goat anti-human IgG antibody was used for antibody-staining. Flow cytometry data for the binding of 4C11 (green lines) to the Env-expressing cell surface in the presence of sCD4 or a CD4 mimic are shown among gated PM1 cells along with a control antibody (anti-human CD19: black lines). Data are representative of the results from a minimum of two independent experiments. The number at the top of each graph shows the mean fluorescence intensity (MFI) of the antibody 4C11.

Table 2
Combination indices (CI) for compound **2** or sCD4 and a CXCR4 antagonist, T140, against an HIV IIIB strain

Combination	HIV strain	CI values at different IC[a]		
		IC_{50}	IC_{75}	IC_{90}
2 + T140	IIIB	0.786	0.713	0.655
sCD4 + T140	IIIB	0.705	0.528	0.400

[a] The multiple-drug effect analysis reported by Chou et al. was used to analyze the effects of combinational uses of compounds.[18] CI <0.9: synergy, 0.9 < CI < 1.1: additivity, CI >1.1: antagonism.

(Table 2).[15] Compound **2** showed a highly remarkable synergistic anti-HIV activity with a co-receptor CXCR4 antagonist, T140,[8a] against an X4-HIV-1 strain, IIIB at various IC values (IC_{50}, IC_{75} and IC_{90}). However, sCD4 exhibited a higher synergistic effect (lower CI values) with T140 (Table 2). The interaction of sCD4 or a CD4 mimic with gp120 would expose the co-receptor-binding site of gp120, and the co-receptor CXCR4 could then easily approach gp120. Thus, an inhibitory effect of a CXCR4 antagonist would be meaningful, and a significant synergistic effect might also be brought about by a combination of sCD4 or a CD4 mimic and T140.

In summary, a series of CD4 mimic compounds were synthesized and evaluated for their anti-HIV activity. Several compounds showed significant anti-HIV activity with relatively low cytotoxicity. SAR studies showed that a certain level of size and electron-withdrawing ability of the substituents at the *p*-position of the phenyl ring are suitable for potent anti-HIV activity. In addition, the treatment of Env-expressing cells with several CD4 mimicking compounds causes a conformational change, exposing the co-receptor-binding site of gp120 externally. Thus, a CD4 mimic exhibited a remarkable synergistic effect with a co-receptor antagonist. These compounds are essential probes directed to the dynamic supramolecular mechanism of HIV entry, and important leads for the cocktail therapy of AIDS.

Acknowledgments

This work was supported by Mitsui Life Social Welfare Foundation, Grant-in-Aid for Scientific Research from the Ministry of Education, Culture, Sports, Science, and Technology of Japan, and Health and Labour Sciences Research Grants from Japanese Ministry of Health, Labor, and Welfare.

References and notes

1. Mitsuya, H.; Erickson, J. In *Textbook of AIDS Medicine*; Merigan, T. C., Bartlett, J. G., Bolognesi, D., Eds.; Williams & Wilkins: Baltimore, 1999; pp 751–780.
2. Chan, D. C.; Kim, P. S. *Cell* **1998**, *93*, 681.
3. (a) Alkhatib, G.; Combadiere, C.; Broder, C. C.; Feng, Y.; Kennedy, P. E.; Murphy, P. M.; Berger, E. A. *Science* **1996**, *272*, 1955; (b) Choe, H.; Farzan, M.; Sun, Y.; Sullivan, N.; Rollins, B.; Ponath, P. D.; Wu, L.; Mackay, C. R.; LaRosa, G.; Newman, W.; Gerard, N.; Gerard, C.; Sodroski, J. *Cell* **1996**, *85*, 1135; (c) Deng, H. K.; Liu, R.; Ellmeier, W.; Choe, S.; Unutmaz, D.; Burkhart, M.; Marzio, P. D.; Marmon, S.; Sutton, R. E.; Hill, C. M.; Davis, C. B.; Peiper, S. C.; Schall, T. J.; Littman, D. R.; Landau, N. R. *Nature* **1996**, *381*, 661; (d) Doranz, B. J.; Rucker, J.; Yi, Y. J.; Smyth, R. J.; Samson, M.; Peiper, S. C.; Parmentier, M.; Collman, R. G.; Doms, R. W. *Cell* **1996**, *85*, 1149; (e) Dragic, T.; Litwin, V.; Allaway, G. P.; Martin, S. R.; Huang, Y.; Nagashima, K. A.; Cayanan, C.; Maddon, P. J.; Koup, R. A.; Moore, J. P.; Paxton, W. A. *Nature* **1996**, *381*, 667.
4. Feng, Y.; Broder, C. C.; Kennedy, P. E.; Berger, E. A. *Science* **1996**, *272*, 872.
5. Wild, C. T.; Greenwell, T. K.; Matthews, T. J. *AIDS Res. Hum. Retroviruses* **1993**, *9*, 1051.
6. (a) Dorr, P.; Westby, M.; Dobbs, S.; Griffin, P.; Irvine, B.; Macartney, M.; Mori, J.; Rickett, G.; Smith-Burchnell, C.; Napier, C.; Webster, R.; Armour, D.; Price, D.; Stammen, B.; Wood, A.; Perros, M. *Antimicrob. Agents Chemother.* **2005**, *49*, 4721; (b) Price, D. A.; Armour, D.; De Groot, M.; Leishman, D.; Napier, C.; Perros, M.; Stammen, B. L.; Wood, A. *Bioorg. Med. Chem. Lett.* **2006**, *16*, 4633.
7. (a) Cahn, P.; Sued, O. *Lancet* **2007**, *369*, 1235; (b) Grinsztejn, B.; Nguyen, B.-Y.; Katlama, C.; Gatell, J. M.; Lazzarin, A.; Vittecoq, D.; Gonzalez, C. J.; Chen, J.; Harvey, C. M.; Isaacs, R. D. *Lancet* **2007**, *369*, 1261.
8. (a) Tamamura, H.; Xu, Y.; Hattori, T.; Zhang, X.; Arakaki, R.; Kanbara, K.; Omagari, A.; Otaka, A.; Ibuka, T.; Yamamoto, N.; Nakashima, H.; Fujii, N. *Biochem. Biophys. Res. Commun.* **1998**, *253*, 877; (b) Fujii, N.; Oishi, S.; Hiramatsu, K.; Araki, T.; Ueda, S.; Tamamura, H.; Otaka, A.; Kusano, S.; Terakubo, S.; Nakashima, H.; Broach, J. A.; Trent, J. O.; Wang, Z.; Peiper, S. C. *Angew. Chem., Int. Ed.* **2003**, *42*, 3251; (c) Tanaka, T.; Nomura, W.; Narumi, T.; Esaka, A.; Oishi, S.; Ohashi, N.; Itotani, K.; Evans, B. J.; Wang, Z.; Peiper, S. C.; Fujii, N.; Tamamura, H. *Org. Biomol. Chem.* **2009**, *7*, 3805.
9. Otaka, A.; Nakamura, M.; Nameki, D.; Kodama, E.; Uchiyama, S.; Nakamura, S.; Nakano, H.; Tamamura, H.; Kobayashi, Y.; Matsuoka, M.; Fujii, N. *Angew. Chem., Int. Ed.* **2002**, *41*, 2937.
10. (a) Zhao, Q.; Ma, L.; Jiang, S.; Lu, H.; Liu, S.; He, Y.; Strick, N.; Neamati, N.; Debnath, A. K. *Virology* **2005**, *339*, 213; (b) Schön, A.; Madani, N.; Klein, J. C.; Hubicki, A.; Ng, D.; Yang, X.; Smith, A. B., III; Sodroski, J.; Freire, E. *Biochemistry* **2006**, *45*, 10973; (c) Madani, N.; Schön, A.; Princiotto, A. M.; LaLonde, J. M.; Courter, J. R.; Soeta, T.; Ng, D.; Wang, L.; Brower, E. T.; Xiang, S.-H.; Do Kwon, Y.; Huang, C.-C.; Wyatt, R.; Kwong, P. D.; Freire, E.; Smith, A. B., III; Sodroski, J. *Structure* **2008**, *16*, 1689; (d) Haim, H.; Si, Z.; Madani, N.; Wang, L.; Courter, J. R.; Princiotto, A.; Kassa, A.; DeGrace, M.; McGee-Estrada, K.; Mefford, M.; Gabuzda, D.; Smith, A. B., III; Sodroski, J. *ProS Pathogens* **2009**, *5*, 1.
11. The structure of compound **2** was built in Sybyl and minimized with the MMFF94 force field and partial charges. (see: Halgren, T. A. *J. Comput. Chem.* **1996**, *17*, 490.) Docking was then performed using FlexSIS through its SYBYL

module, into the crystal structure of gp120 (PDB, entry 1RZJ). The binding site was defined as residues Val^{255}, Asp^{368}, Glu^{370}, Ser^{375}, Ile^{424}, Trp^{427}, Val^{430} and Val^{475}, and included residues located within a radius 4.4 Å. The ligand was considered to be flexible, and all other options were set to their default values. Figures were generated with ViewerLite version 5.0 (Accelrys Inc., San Diego, CA).

12. *For example, the synthesis of compound* **7**: To a solution of ethyl oxalyl chloride (0.400 mL, 3.48 mmol) in THF (20 mL) were added triethylamine (Et_3N) (0.480 mL, 3.48 mmol) and *p*-toluidine (373 mg, 3.48 mmol) with stirring at 0 °C. The reaction mixture was allowed to warm to room temperature, and then stirred for 6 h. After removal by filtration of the resulting salts, the filtrate was concentrated under reduced pressure. The residue was extracted with EtOAc (50 mL), and the extract was washed successively with brine (20 mL), 1 M HCl (20 mL × 2), brine (20 mL), saturated $NaHCO_3$ (20 mL × 2) and brine (20 mL × 3), then dried over $MgSO_4$. Concentration under reduced pressure gave the crude ethyl oxalamate, which was used without further purification. To a solution of the crude ethyl oxalamate (640 mg, 3.09 mmol) in THF (30 mL) were added aqueous 1 M NaOH (3.40 mL, 3.40 mmol), water (50 mL) and MeOH (20 mL) with stirring at 0 °C. The reaction mixture was allowed to warm to room temperature, and then stirred for 20 h. After the addition of aqueous 1 M HCl (5 mL), MeOH and THF were evaporated under reduced pressure. The residue was acidified to pH 2 with 1 M HCl, and extracted with EtOAc (50 mL × 2). The combined organic layer was washed with brine (20 mL × 3), and dried over $MgSO_4$. Concentration under reduced pressure gave the crude acid, which was used for the next reaction without further purification. To a solution of the above crude acid (514 mg, 2.87 mmol) in THF (10 mL) were added 1-hydoxybenzotriazole (484 mg, 3.16 mmol), 4-amino-2,2,6,6-tetramethylpiperidine (446 μL, 2.58 mmol), 1-ethyl-3-(3-dimethylaminopropyl)carbodiimide hydrochloride (606 mg, 3.16 mmol) and Et_3N (0.439 mL, 3.16 mmol) with stirring at 0 °C. The reaction mixture was allowed to warm to room temperature, and then stirred for 20 h. After evaporation of THF, the residue was dissolved in $CHCl_3$ (50 mL). The mixture was washed with saturated $NaHCO_3$ (20 mL × 2) and brine (20 mL × 3), and dried over $MgSO_4$. Concentration under reduced pressure gave the crude crystalline mass. The usual work-up followed by recrystallization from EtOAc–*n*-hexane gave the title compound **7** (363 mg, 1.14 mmol, 39.8%) as colorless crystals, mp = 176 °C; δ_H (400 MHz; $CDCl_3$) 1.07 (1H, m, NH), 1.16 (6H, s, CH_3), 1.29 (6H, s, CH_3), 1.44 (2H, m, CH_2), 1.91 (1H, d, *J* 3.7, C*H*H), 1.94 (1H, d, *J* 3.7, CH*H*), 2.34 (3H, s, CH_3), 4.25 (1H, m, CH), 7.17 (2H, d, *J* 8.3, ArH), 7.33 (1H, m, NH), 7.50 (2H, d, *J* 8.4, ArH), 9.18 (1H, s, NH); HRMS (FAB), *m*/*z* calcd for $C_{18}H_{28}N_3O_2$ $(MH)^+$ 318.2182, found 318.2173.
13. McFarland, C.; Vicic, D. A.; Debnath, A. K. *Synthesis* **2006**, 807.
14. *The synthesis of compound* **12**: To a solution of Et_3N (417 μL, 3.00 mmol) and 4-nitroaniline (138 mg, 1.00 mmol) in THF (1.3 mL) was added oxalyl dichloride (85.8 μL, 1.00 mmol) with stirring at 0 °C. After being stirred for 30 min at 0 °C, Et_3N (167 μL, 1.20 mmol) and 4-amino-2,2,6,6-tetramethylpiperidine (156 μL, 0.90 mmol) were added. The reaction mixture was stirred for 6 h at 0 °C. After removal by filtration of the resulting salts, the filtrate was concentrated under reduced pressure. The residue was dissolved in $CHCl_3$ (20 mL), and the mixture was washed successively with brine (10 mL), saturated $NaHCO_3$ (10 mL × 2) and brine (10 mL × 3), and dried over $MgSO_4$. Concentration under reduced pressure followed by flash chromatography over silica gel with $CHCl_3$–MeOH (9:1) gave 42.4 mg (0.122 mmol, 13.5%) of the title compound **12** as colorless crystals, mp = 190 °C; δ_H (400 MHz; $CDCl_3$) 1.09 (1H, m, NH), 1.17 (6H, s, CH_3), 1.29 (6H, s, CH_3), 1.43 (2H, m, CH_2), 1.92 (1H, d, *J* 3.8, C*H*H), 1.95 (1H, d, *J* 3.8, CH*H*), 4.28 (1H, m, CH), 7.29 (1H, m, NH), 7.82 (2H, d, *J* 9.1, ArH), 8.28 (2H, d, *J* 9.1, ArH), 9.55 (1H, s, NH); HRMS (FAB), *m*/*z* calcd for $C_{17}H_{25}N_4O_4$ $(MH)^+$ 349.1876, found 349.1871.
15. Yoshimura, K.; Shibata, J.; Kimura, T.; Honda, A.; Maeda, Y.; Koito, A.; Murakami, T.; Mitsuya, H.; Matsushita, S. *AIDS* **2006**, *20*, 2065.
16. (a) Chapman, N. B.; Shorter, J. *Advances in Linear Free Energy Relationship*; Plenum Press: London, 1972; (b) Chapman, N. B.; Shorter, J. *Correlation Analysis in Chemistry*; Plenum Press: London, 1978; (c) Hansch, C.; Leo, A. J.; Hoekman, D. *Exploring QSAR, Hydrophobic, Electronic, and Steric Constants*; American Chemical Society: Washington, DC, 1995.
17. Taft, R. W. In *Steric Effects in Organic Chemistry*; Newman, M. S., Ed.; John Wiley: New York, 1956; p 556.
18. (a) Chou, T. C.; Talalay, P. *J. Biol. Chem.* **1977**, *252*, 6438; (b) Chou, T. C.; Hayball, M. P. *CalcuSyn*, 2nd ed.; Biosoft: Cambridge, UK, 1996.

JGV Papers in Press. Published December 23, 2009 as doi:10.1099/vir.0.017426-0

HIV-1 evasion of a neutralizing anti-V3 antibody involves acquisition of a potential glycosylation site in V2.

Makiko Hatada, Kazuhisa Yoshimura, Shigeyoshi Harada, Yoko Kawanami, Junji Shibata and Shuzo Matsushita*

Division of Clinical Retrovirology and Infectious Diseases, Center for AIDS Research, Kumamoto University, Kumamoto 860-0811, Japan

Running title: Neutralizing antibody evasion of HIV-1

*Corresponding author:

Shuzo Matsushita

Division of Clinical Retrovirology and Infectious Diseases, Center for AIDS Research, Kumamoto University, Kumamoto 860-0811, Japan

Phone: +81-96-373-6536

Facsimile: +81-96-373-6537

E-mail: shuzo@kumamoto-u.ac.jp

Summary: 240 words, Main text: 5459 words, 6 figures, 2 tables and 1 supplementary data.

21 **Summary**

22 It has been reported that the addition of a potential N-linked glycosylation site (PNGS)
23 to the gp120 HIV-1 envelope glycoprotein provides protection against neutralizing
24 antibodies (NAbs) by acting as a 'glycan shield'. In this study, we induced insertion of a
25 PNGS in the V2 region of HIV-1_{BaL} with the KD-247 anti-V3 neutralizing monoclonal
26 antibody. In the presence of KD-247 (200 $\mu g\ ml^{-1}$) at passage five, viruses with three
27 amino acid mutations in the C2 (T240S and I283T) and V3 (T319A) regions expanded
28 from pre-existing variants. After six passages with KD-247 (> 300 $\mu g\ ml^{-1}$), a PNGS
29 emerged in the V2 region in addition to C2 (T240S) and V3 mutations (R315K and
30 F317L). A variant with a PNGS insertion in V2 but no V3 mutations was sensitive to
31 KD-247, whereas a clone with a V2 PNGS insertion and mutations in V3 demonstrated
32 a high level of resistance to KD-247. Replication kinetics analysis revealed that the
33 F317L mutation in V3 played a compensatory role for fitness-loss caused by the PNGS
34 insertion in V2. The evading HIV-1 variant did not revert back to the wild-type virus
35 after 14 passages without KD-247. These findings demonstrate that the virus with
36 fitness-loss mutations can replicate equally as well as the wild-type virus to acquire
37 some key mutations in the V3 stem and the C2 region, and the compensated variants
38 containing PNGS do not revert back to the ancestral virus even in the absence of NAb.

Introduction

A neutralizing antibody (NAb) against human immunodeficiency virus type 1 (HIV-1) is an essential component of a protective vaccine. However, primary isolates of HIV-1 are relatively resistant to neutralization compared with variants selected for growth in permanent cell lines (Moore *et al.*, 1995; Pugach *et al.*, 2004). Studies addressing differences between neutralization-sensitive and -resistant variants have revealed several mechanisms that are responsible for neutralization resistance in primary isolates. These mechanisms include the occlusion of epitopes within the envelope glycoprotein (Env) oligomer and the extensive glycosylation and extension of variable loops from the surface of the complex leading to steric and conformational blocking of receptor binding sites (Kwong *et al.*, 2002; McCaffrey *et al.*, 2004; Pinter *et al.*, 2004; Saunders *et al.*, 2005). The structural features of one envelope glycoprotein, Env gp120, means that it can tolerate a vast array of mutations permitting the selection of neutralization evading variants, as has been previously demonstrated in culture assays, animal models and infected individuals (Johnson & Desrosiers, 2002).

Although there is ample data showing that NAbs can protect against HIV-1 infection *in vitro* and *in vivo*, their activity in infected humans remains controversial (Cao *et al.*, 1995; Deeks *et al.*, 2006; Montefiori *et al.*, 2001; Sullivan *et al.*, 1993). Passive transfer

of a combination of broadly neutralizing monoclonal antibodies (MAbs) 2G12, 2F5 and 4E10 in patients during a structured treatment interruption resulted in a significant delay in viral rebound in some patients compared with viral rebound in the absence of these antibodies (Trkola *et al.*, 2005). This would indicate that viral suppression was because of the antiviral activity of the administered antibodies. Subsequent studies addressing the pharmacokinetics of each MAb (Joos *et al.*, 2006), neutralization-resistance mutations (Manrique *et al.*, 2007) and protective neutralization titres *in vivo* (Trkola *et al.*, 2008) using samples from the study further supported the protective effects of NAb *in vivo*.

Clinical studies examining NAbs in primary infections have suggested that the majority of recently infected individuals mount a vigorous antibody response against autologous virus. However, the rapid evolution of HIV in the presence of NAb results in the emergence of evading mutants. As a consequence, at any time during the early stages of HIV infection, NAbs are more likely to recognize earlier form of the viruses as opposed to recent variants. Despite evidence of phenotypic resistance, the genetic basis of the mechanism allowing primary viruses to evade NAbs is poorly understood.

Wei *et al.* found that glycosylation of Env plays an important role in evading neutralization. The evolving 'glycan shield' can sterically block antibody binding

without mutation at the antibody-binding site (Wei *et al.*, 2003). Also, insertion of potential N-linked glycosylation sites (PNGSs) along with other mutations has been associated with viral evasion of NAbs (Bunnik *et al.*, 2008; Wei *et al.*, 2003). Conversely, Frost *et al.* reported that viral evasion of NAb correlates to the rate of amino acid substitution rather than changes in glycosylation and insertions or deletions in Env (Frost *et al.*, 2005). This would suggest that the individual contribution of PNGSs to the neutralization sensitivity of HIV-1 depends on the presence of other mutations in the Env sequence. However, the relationship between PNGSs and mutations of NAb resistance has not been investigated because of technical difficulties resulting from the polyclonal nature of NAbs and the primary isolates used in previous clinical studies. To clarify the genetic mechanisms responsible for evading neutralization, it is important to analyse individual mutations resulting from neutralization evasion of NAbs in an *in vitro* culture system.

Neutralization evasion from anti-V3 MAbs has been reported and associated with amino acid substitution within the epitope of the V3 loop and outside V3 (Gorny *et al.*, 2004; Masuda *et al.*, 1990; Park *et al.*, 1998; Pinter *et al.*, 2004; Shibata *et al.*, 2007; Yoshimura *et al.*, 2006; Zolla-Pazner, 2004). However, the role(s) of PNGSs in

92 resistance to neutralization is not clear because the induction of PNGSs under
93 neutralizing MAbs pressure *in vitro* has not been reported.

94 In this study, we obtained evasion mutants harbouring PNGSs in the V2 region and
95 mutations in the C2 and V3 regions, during induction of neutralization evasion mutants
96 from anti-V3 MAb KD-247 in HIV-1_{BaL}. KD-247 is a humanized MAb that
97 demonstrates cross-neutralizing activity against HIV-1 isolates in clade B. The epitope
98 of KD-247 was mapped to six amino acids, IGPGRA, at the tip of the V3 loop (Eda *et*
99 *al.*, 2006). A series of analyses using viral clones that have corresponding mutations
100 present in evading viruses revealed a mutant that has both a PNGS-insertion in V2 and
101 mutations in V3 along with a highly resistant phenotype to the NAb. However, the
102 mutant requires further mutation to compensate for reduced replication ability. Studies
103 to elucidate replication kinetics indicated that the F317L mutation in V3 and the T240S
104 mutation in C2 play a key role in maintaining resistant mutations in V2 and V3, which
105 were related to the fitness-loss. Our study partially explains the complex nature of the
106 development of neutralization resistance observed in previous clinical studies.
107

Results

Selection of anti-V3 MAb KD-247 evasion mutants from HIV-1_{BaL}

To select a HIV-1 variant able to evade neutralization by KD-247 *in vitro*, we exposed PM1/CCR5 cells to HIV-1_{BaL} and serially passaged the virus in the presence of increasing concentrations of KD-247. PM1/CCR5 cells were highly sensitive to both X4 and R5 HIV-1 infection, displaying prominent syncytia (Yusa *et al.*, 2005). As a control, HIV-1_{BaL} was passaged under the same conditions without MAb to monitor spontaneous changes that occurred in the virus during prolonged PM1/CCR5 cell passage (denoted as passage control). Because HIV-1_{BaL} was sensitive to neutralization by KD-247 with an IC_{50} of 3.8 μg ml^{-1} as determined by MTT assay (data not shown), the selected virus was initially propagated in the presence of 5 μg ml^{-1} KD-247. During the course of the selection procedure, the MAb concentration was increased to 2,000 μg ml^{-1}. Following five rounds of passage (p5), a viral variant designated HIV-1_{BaL} (200) p5, arose that replicated in the presence of 200 μg ml^{-1} KD-247. After passage 16, a viral variant designated HIV-1_{BaL} (2000) p16, arose that infected PM1/CCR5 cells efficiently in the presence of 2,000 μg ml^{-1} KD-247. We harvested viruses at six passages (p2, p5, p6, p7, p10 and p16) as well as a baseline virus, HIV-1_{BaL} (0) p0, and a passage control designated HIV-1_{BaL} (0) p10. These viruses were evaluated for their sensitivity to

KD-247 using TZM-bl as target cells (Table 1). The IC_{50} values of KD-247 against HIV-1_{BaL} (0) p0, HIV-1_{BaL} (200) p5, HIV-1_{BaL} (300) p6 and HIV-1_{BaL} (2000) p16 were 0.32 ± 0.2 $\mu g\ ml^{-1}$, 5.68 ± 1.48 $\mu g\ ml^{-1}$, > 100 $\mu g\ ml^{-1}$ and > 100 $\mu g\ ml^{-1}$ respectively, indicating that HIV-1_{BaL} acquired a resistant phenotype against KD-247 during *in vitro* selection. At passage 5, HIV-1_{BaL} acquired a moderately resistant phenotype and after passage 6, the virus had developed a highly resistant phenotype.

DNA sequence of the envelope region of evasion mutants

To determine the genetic basis of resistance in the variant HIV-1_{BaL} strains, the C1 to C4 region of the env gene was amplified from genomic DNA extracted from the infected cells, cloned and sequenced (Fig. 1).

At passage 5, moderately resistant variants with T240S, I283T and T319A mutations were in the majority. However, the proportion of variants decreased gradually as the KD-247 concentration was increased (Fig. 1B and Fig. 2E). This observation suggests that at low concentrations of KD-247, the variants with moderate resistance to the anti-V3 MAb are selected from the pre-existing variants.

Insertion of a PNGS in the V2 region and an amino acid substitution at the V3 tip (R315K) were observed at passages 5 and 6, respectively. Both of these alterations were